15

Method for determining the depth of deposit of gamma-ray radiation sources using a xenon gamma-ray spectrometer

© A.I. Madzhidov, K.F. Vlasik, V.M. Grachev, V.V. Dmitrenko, K.V. Krivova, S.E. Ulin, Z.M. Uteshev, A.E. Shustov, M.D. Timashkova

National Research Nuclear University „MEPhI“, Moscow, Russia
e-mail: aimadzhidov@mephi.ru

Received November 11, 2024
Revised January 22, 2025
Accepted February 5, 2025

Radioactive contamination of nuclear-physical facilities is a serious obstacle to their operation and decommissioning. In this article, a method for determining the depth of deposit of radioactive sources based on the analysis of energy gamma-spectra, calculation of the ratio of the area of the peak of total absorption to the area of the Compton valley is proposed. The proposed method is tested on various adsorbents using a xenon gamma-spectrometer as a registering device.

Keywords: gamma-radiation, Compton valley, gamma-spectrometer, xenon.

DOI: 10.61011/TP.2025.06.61390.415-24

Introduction

The use of gamma-ray spectrometers with high energy resolution and high light intensity makes it possible to significantly improve the information content and effectiveness of gamma-ray spectrometric methods in scientific research and applied fields. Currently, gamma-ray spectrometers based on ultrapure germanium (HPGe) are mainly used, providing a high energy resolution of 0.2

The necessary initial stage of radioactive waste management is the process of its sorting, which should provide data on the intensity of radiation and the composition of the dominant radioisotopes. Taking into account the conditions of various industries (NFC, NPP, NWC, production of radioactive isotopes), to solve this problem it is advisable to use gamma-ray spectrometers with high energy resolution, capable of operating in a wide temperature range exposed to intense ionizing radiation fields, with a large operational resource, short measurement time and, if possible, without any special cooling systems that complicate and increase the cost of their operation.

Despite the fact that there are many radioactive fission products, most of these isotopes decay quite quickly. The basic long-living radionuclides include ^{137}Cs, ^{60}Co, ^{133}Ba, ^{152}Eu and etc. Of course, such elements can be found in the form of radioactive waste, leaks or emissions after accidents of nuclear power plants under the ruins of layers of structures or earth.

There is a need to accurately determine the type of radionuclide and its depth of occurrence. To solve this problem, a cadmium telluride (CdTl) semiconductor gamma detector can be used. This type of semiconductor gamma detector makes it possible to detect both gamma quanta and X-rays, with respect to which it is possible to determine the depth of occurrence of radioactive sources emitting in two energy ranges [1]:

$$d = \frac{1}{\mu_X - \mu_Y} \log_e \frac{(N_{0X}/N_{0\gamma})}{(N_X/N_\gamma)}, \qquad (1)$$

where μ_X and μ_γ — X-ray and gamma radiation absorption coefficients, N_{0X} and $N_{0\gamma}$ — counting rates of X-ray and gamma photo peaks at zero depth, N_X and N_γ — rate of counting at the studied depth d of the source occurrence.

A CdTl semiconductor-based gamma detector was used to measure the spectrum of ^{137}Cs isotope, which was located in quartz sand (Fig. 1). According to the measurement results, the ratio of the counting rate $\log_e N_0/N_{X/\gamma}$ was obtained from the depth of d occurrence (Fig. 1, *c*).

The X-ray photopeak observed at a depth of 5 mm is absent at a depth of 50 mm, whereas the peak from the gamma-ray quantum with an energy of 662 keV is present at both depths, but is significantly attenuated at a depth of 50 mm compared to a depth of 5 mm by approximately 50%.

Estimates of the uncertainty associated with determining the depth of the source based on these calibration data show that depth estimates can be made with an accuracy of ± 1 mm. The disadvantage of this study is that the amplitude of X-ray photopic declines with higher thickness of the absorber, which leads to the inapplicability of this method for large thicknesses.

Research of this type was also made with HPGe [2]. In this experiment, several layers of concrete tiles were used as an absorber, the source of gamma rays was ^{152}Eu (Fig. 2).

To determine the source depth, the method of the ratio of the full absorption peak area to the area of the Compton valley was also used, which compares the counting rate of the peak of full absorption measured by a portable HPGe and the counting rate of the Compton valley. Using the

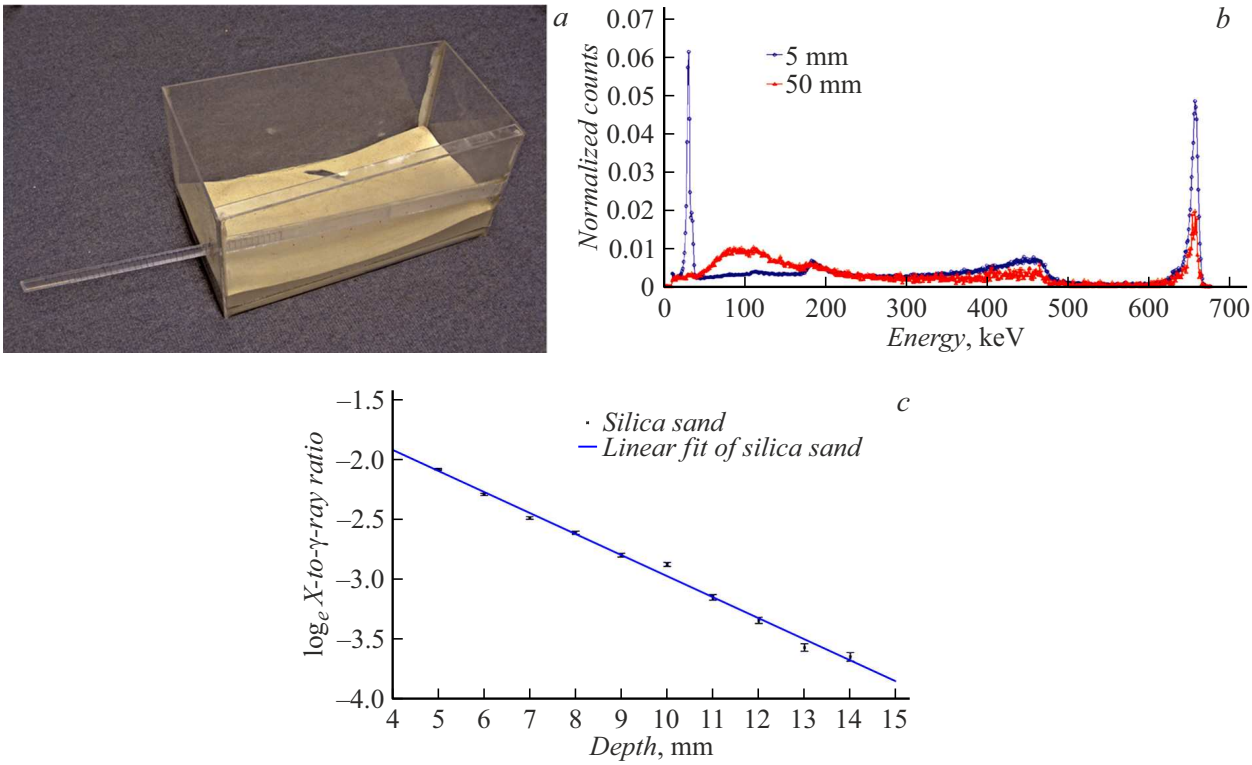

Figure 1. *a* — photo of a phantom filled with sand (silicon) containing radioisotope ^{137}Cs, *b* — two spectra for a closed point source ^{137}Cs placed at a depth of 5 and 50 mm in quartz sand, *c* — graph of the dependence of $\log_e N_0/N_{X/\gamma}$ on depth *d* for a point source immersed in dry quartz sand.

results of this study, it is possible to estimate the depth of the gamma radiation source with a relative error of about 20%. Among the drawbacks of this study are the high cost of the HPGe crystal detector and the need to cool it during operation.

1. Experimental setup

An integral part of the xenon gamma spectrometer (XGS) is a xenon gamma detector (CGD) based on a cylindrical ionization chamber filled with a mixture of compressed xenon and hydrogen with a shielding grid operating in the pulsed mode [3–6]. The working volume of the gamma detector is 2000 cm^3 with an end area of 430 cm^2. The ratio of the working volume of the ionization chamber to the total volume of the detector is approximately 85%. The general view of XGD is shown in Fig. 3.

The physical and technical characteristics of the xenon gamma detector are presented in Table 1.

To study the spectrometric characteristics of XGS, spectra from photon radiation sources of MSGS type (model spectrometric gamma radiation sources) with an activity of no more than 100 kBq were collected. When measuring the spectra, the gamma sources were located at a distance of 20 cm from the end of XGD. A digital electronics unit developed in NRNU MEPhI was used to process electrical pulses from XGD and accumulate energy spectra of the detected gamma radiation. A personal computer with a specialized software installed, also developed in NRNU MEPhI, was used to analyze the operation of XGS and process data in real time.

As an example, Figure 4 shows the characteristic spectra from gamma sources ^{137}Cs, ^{133}Ba, ^{60}Co and ^{152}Eu, measured by a xenon gamma-ray spectrometer.

To determine the minimum detectable activity (MDA) of XGS the spectra from gamma-ray sources of MSGS type were measured. The sources are located from the end of the detector at a distance of 26 cm from the center of the XGS for 1000 s. The measurement results are presented in Table 2.

2. Measurement method

Previously, using XGS the occurrence depth of ^{137}Cs gamma-quanta source for various soil thicknesses was investigated [7], where the experimental technique was based on a change in the peak of full absorption and Compton valley in the obtained gamma-ray spectra.

To study the absorption of gamma rays in ceramic tiles, KGS spectra from various gamma sources were

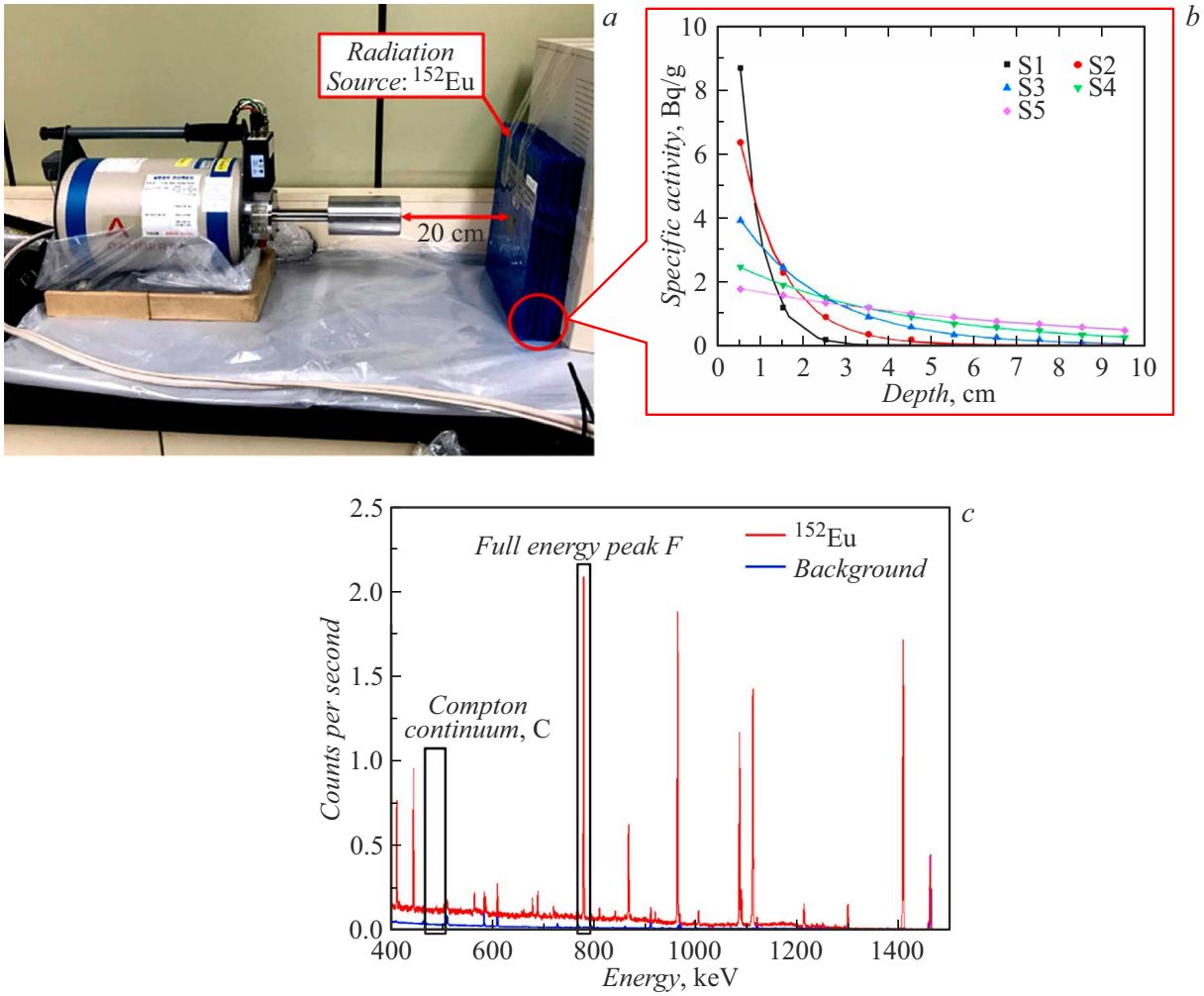

Figure 2. *a* — HPGe gamma spectrometer and concrete tiles, *b* — graph of specific activity dependences on absorber thicknesses for concrete tile sets S1-5, *c* — gamma spectrum obtained from radionuclide ^{152}Eu by means of HPGe gamma-ray spectrometer.

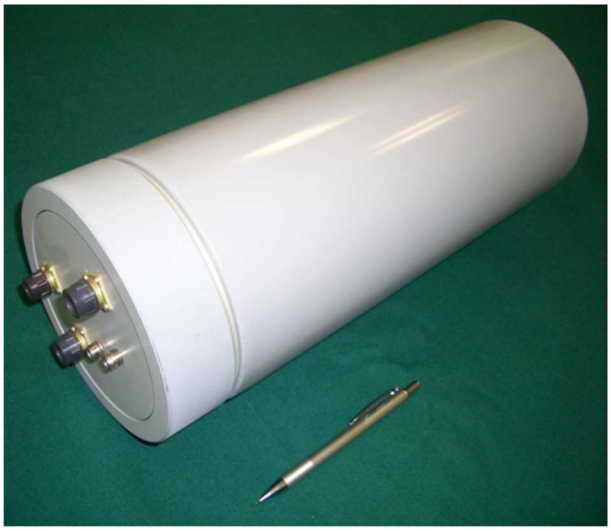

Figure 3.

measured. The chemical composition of the ceramic tile was determined using an X-ray fluorescence spectrometer (Table 3) [8].

Information about chemical composition of ceramics were put in XMuDat software [9], that allowed to get the absorption coefficient for this ceramics.

3. Experimental results

Experimental studies were conducted, where from one to twelve ceramic tiles 20 × 15 × 0.65 cm in size were placed in front of the end of the XGS. Gamma-sources of MSGS type (^{60}Co, ^{137}Cs, ^{133}Ba and ^{152}Eu) were used located before ceramic tiles (Fig. 5).

Figure 6 shows the energy spectra of gamma sources ^{60}Co, ^{137}Cs, ^{133}Ba and ^{152}Eu measured by XGS in the presence of ceramic tiles, where the spectrum of background gamma radiation has been deducted.

Table 1. Main technical characteristics of XGD

Parameter and units of measure	Parameter value
Density of xenon, g/cm^3	0.3–0.4
Pressure of xenon at 23°C, atm	42
Range of the measured energies of gamma-quanta, MeV	0.04–3
Energy resolution for gamma-ray energy 662 keV, %	1.9 ± 0.3
Efficiency of gamma-ray detection with energy of 662 keV, %	2
Linearity of energy scale, %	< 1
Sensitive volume, cm^3	2000
Voltage on detector grid, kV	13
Voltage on detector cathode, kV	21
Anode diameter, mm	20
Anode diameter, mm	40
Cathode diameter, mm	117
Thickness of detector wall, mm	3
Weight, kg	5
Dimensions, cm	Ø15 × 45
Energy supply, W	no more than 25
Power voltage, V	$\sim$ 220 or +27
Operating temperature range (without temperature control system), °C	from 0 to +90
Service life, years	not less than 10
Radiation resistance, ability to operate at neutron fluxes, neutron/c · cm^2	40

With an increase in the number of ceramic tiles, a relative increase in the area of the Compton valley is clearly observed, which was selected in the range of gamma-quanta energies for the source ^{60}Co from 1200 to 1280 keV, ^{137}Cs from 500 to 600 keV, ^{133}Ba from 310 to 335 keV and ^{152}Eu from 255 to 325 keV. For ^{137}Cs source, the range selected for the Compton valley is located between the peak of full absorption and the right edge of Compton distribution, taking into account peak broadening and boundary blurring. For ^{60}Co, ^{133}Ba and ^{152}Eu the range was selected similar to that which was taken by the authors in [2], where there were no high absorption peaks.

After processing of experimental data, the absorption coefficients of ceramics were obtained depending on the energy of gamma quanta (Fig. 7).

Based on the results of the experiment (Fig. 7), the absorption coefficient of ceramic tiles was determined, which coincides within the error limits with the tabular values obtained using XMuDat program (Table. 4).

For each spectrum, the counting rates of the full absorption peaks and the Compton valley of various gamma sources were calculated (Fig. 8).

The ratios of the counting rates of full absorption peaks and the Compton valley (S_{Peak}/S_{valley}) were determined depending on the thickness of ceramic tiles (Fig. 9). The area of the Compton valley was calculated in the above ranges, and the peaks of full absorption were approximated by the Gaussian distribution.

To approximate the points in the graphs in Fig. 9, the function was used:

$$y = \Delta e^{-xt}, \quad (2)$$

where Δ — is a constant that determines the ratio of the counting rate of the full absorption peak area and the counting rate of Compton valley area for zero thickness of the absorber, t — is the attenuation coefficient of gamma ray fluxes, which make up the spectrum in the region of the full absorption peak and Compton valley, x — thickness of the absorber.

Errors S_{Peak}/S_{valley} were found by the formula

$$E_{err} = \sqrt{(S^{err}_{Peak}/S_{valley})^2 + \left(S_{Peak}S^{err}_{valley}/(S_{valley})^2\right)^2}, \quad (3)$$

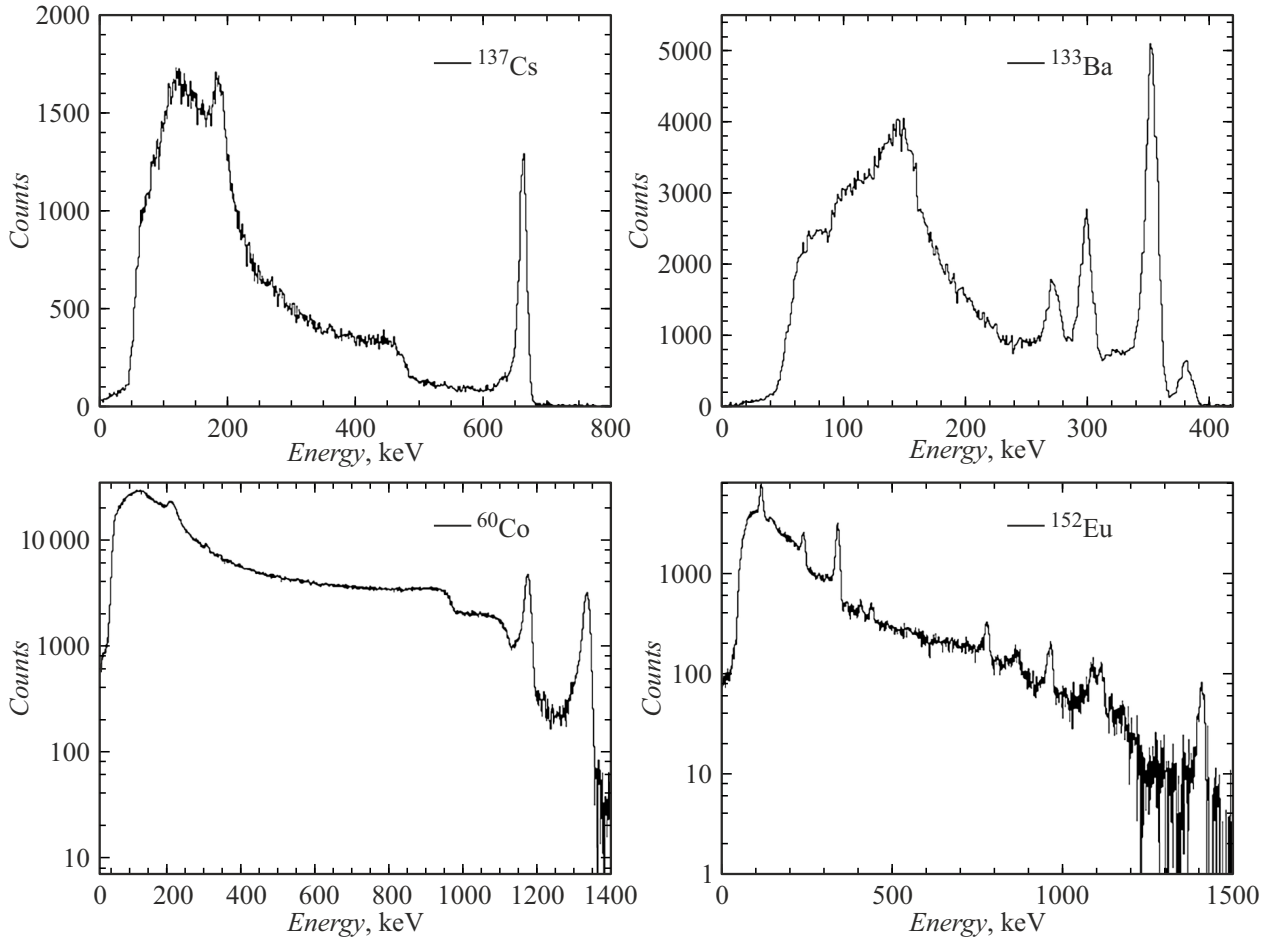

Figure 4. Spectra from ^{137}Cs, ^{133}Ba, ^{60}Co and ^{152}Eu sources obtained when measuring from the edge of XGD.

Table 2. Minimal detected activity of XGS

Isotope	Energy of gamma-quanta, keV	MDA, kBq
^{137}Cs	662	0.26
^{60}Co	1174	1.1
^{60}Co	1332	0.5
^{133}Ba	276	1.13
^{133}Ba	302	1
^{133}Ba	356	0.51
^{133}Ba	386	5.2
^{152}Eu	122	1.89
^{152}Eu	244	4.07
^{152}Eu	344	0.71
^{152}Eu	779	2.46
^{152}Eu	964	5.18
^{152}Eu	1408	2.5

Table 3. Chemical composition of ceramic tile

Components	Relative weight
Silicon dioxide	0.6639
Calcium oxide	0.0364
Aluminum oxide	0.1814
Iron oxide	0.0379
Magnesium oxide	0.036
Potassium oxide	0.0339

where $S_{Peak}S^{err}$ and $S_{valley}S^{err}$ — errors of the full absorption peak area and Compton valley area, S_{Peak} and S_{valley} — areas of the full absorption peak and Compton valley.

Figure 10 shows graphs of the ratio of the full absorption peak area counting rate for gamma-ray energy 662 keV to the rate of Compton valley counting rate versus thickness of various absorbers (ceramics, aluminum, soil, water) obtained from experiments.

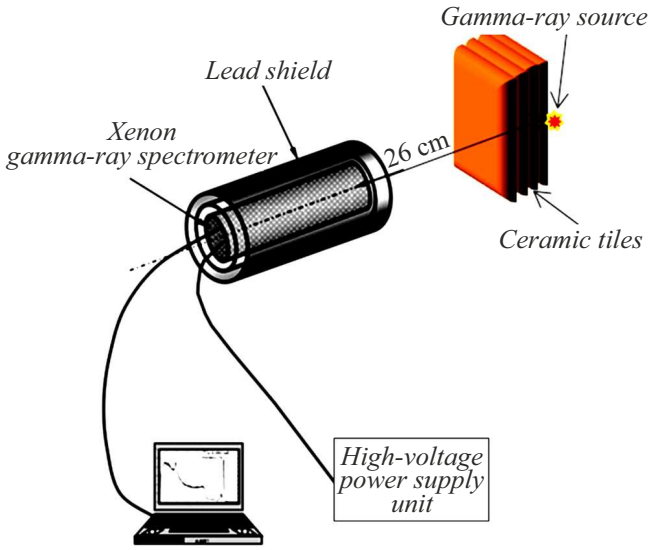

Figure 5. Geometry of experiment.

To calculate the error depth x of the source, the formula is used(2) and its differential:

$$dy = -\Delta t e^{-xi} dx,$$

$$dx = -\frac{dy}{\Delta t} e^{xi}. \quad (4)$$

The error of depth dx depends not only on statistic error dy of the peak−valley ratio, but of the value x itself as well. Due to the peculiarities of the dependence (2), the slope of the tangent to the exponent at large depths x will tend to zero, which leads to higher error. Alternatively, we can use a modified technique to determine the depth from [10], in which the authors, after some transformations, obtain a linear dependence of the inverse normalized peak−valley ratio on the thickness of the absorber. As a result, the error is calculated using a simpler formula:

$$dx = \frac{dy}{A}, \quad (5)$$

where A — linear dependence constant $y = Ax + B$, y — ratios of experimental peak −valley value at a depth of$x = 0$ to the current value of peak−valley at a depth of x (Fig. 11).

Table 5 shows the results of calculations of the depth error of a radioactive source ^{137}with an activity of 100 kBq over a measurement time of 60 min for various materials.

The experimental results and results of Monte Carlo simulation using Geant4 [11] library package were also compared, taking into account the design characteristics of XGS corresponding to a real measuring system. Gamma-ray quanta with an energy of 662 keV were used in modeling. Based on the modeling results ob-

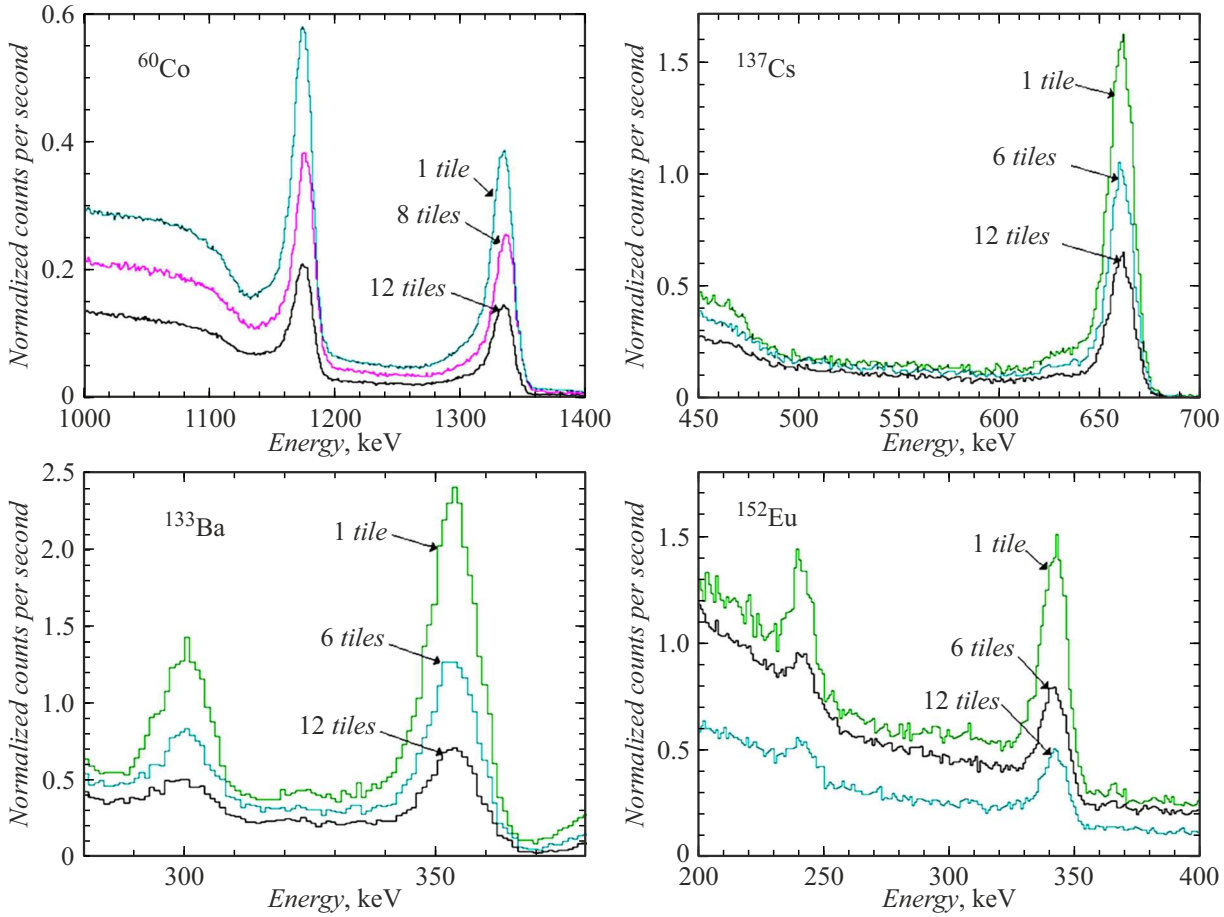

Figure 6. Spectra from ^{60}Co, ^{137}Cs, ^{133}Ba and ^{152}Eu sources with absorbers (ceramics) of various thickness.

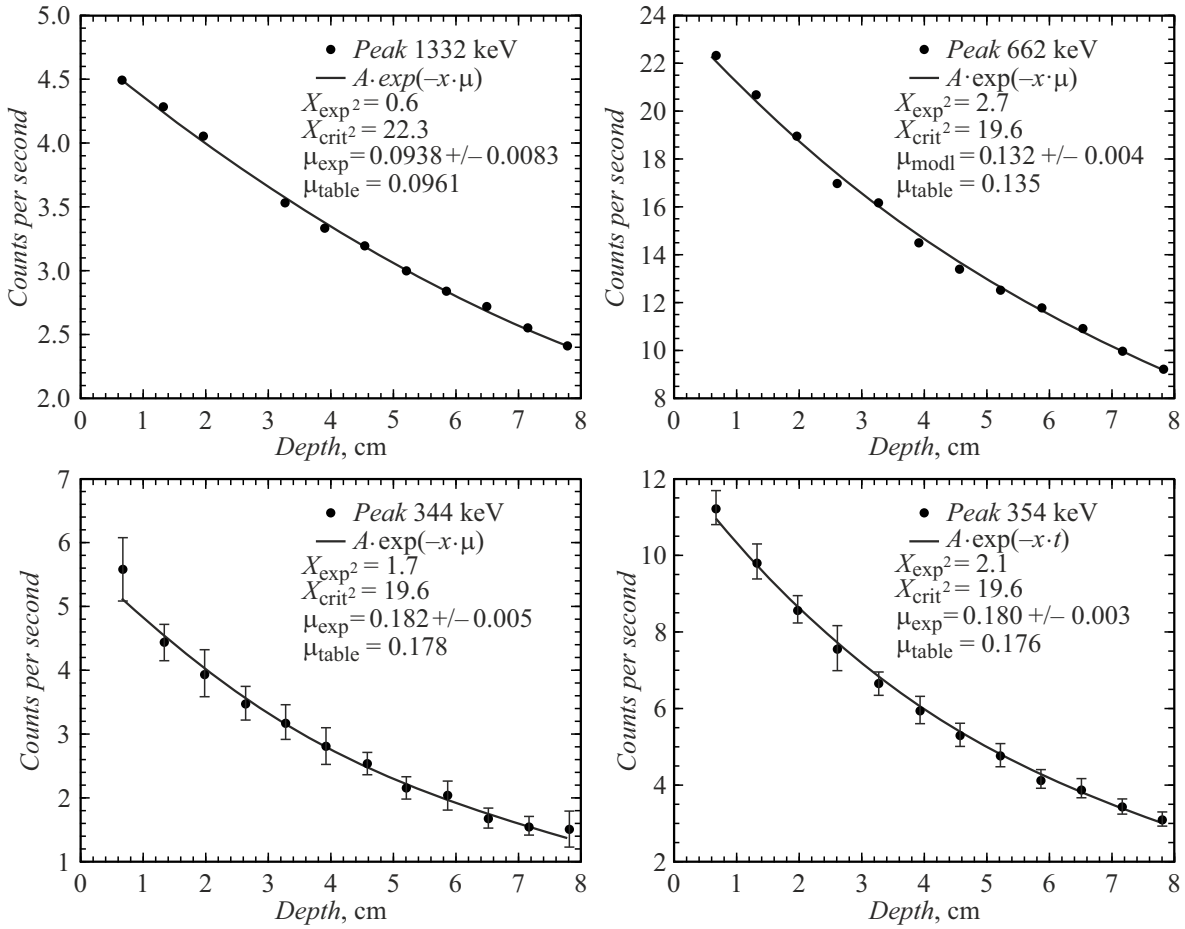

Figure 7. Graphs of full absorption peak area counting rate versus absorber thickness (ceramics) for various gamma-quanta sources — ^{60}Co, ^{137}Cs, ^{133}Ba, ^{152}Eu. χ^2_{exp} and χ^2_{crit} — experimental and critical values of Pierson criteria, μ_{exp} and μ_{table} — experimental and table values of the absorption coefficient.

Table 4. Absorption coefficients of ceramic tiles for different gamma line energies

Gamma source	Energy, keV	Table values of absorption coefficient for ceramics, cm^{-1}	Experimental values of absorption coefficient for ceramics, cm^{-1}
^{60}Co	1332	0.0961	0.094 ± 0.008
^{137}Cs	662	0.1350	0.135 ± 0.004
^{133}Ba	354	0.1760	0.180 ± 0.003
^{152}Eu	344	0.1780	0.182 ± 0.005

tained, a graph was plotted showing the ratio of the full absorption peak area to the area of Compton valley (Fig. 12).

Figure 12 shows that the experimental results and the results obtained using Monte Carlo method in Geant4 program coincide within the error limits.

Conclusion

According to experiments with XGS with a working volume of 2000 cm^3 and gamma sources ^{137}Cs, ^{60}Co, ^{133}Ba, ^{152}Eu, located downstream different absorbers, it was demonstrated that the presented technique using the ratio of the counting rate of the full absorption peak area to the Compton valley area makes it possible to determine the activity, radionuclide composition and depth of radionuclides. The error of the occurrence depth of ^{137}Cs source for ceramics makes 0.32 cm at a depth of 7.8 cm, aluminum 0.58 cm at a depth of 5.3 cm, soil 0.35 cm at a depth of 20 cm and water 0.33 cm at a depth of 12 cm. This technique can be used in the operation and decommissioning of nuclear facilities, in conducting radioe-

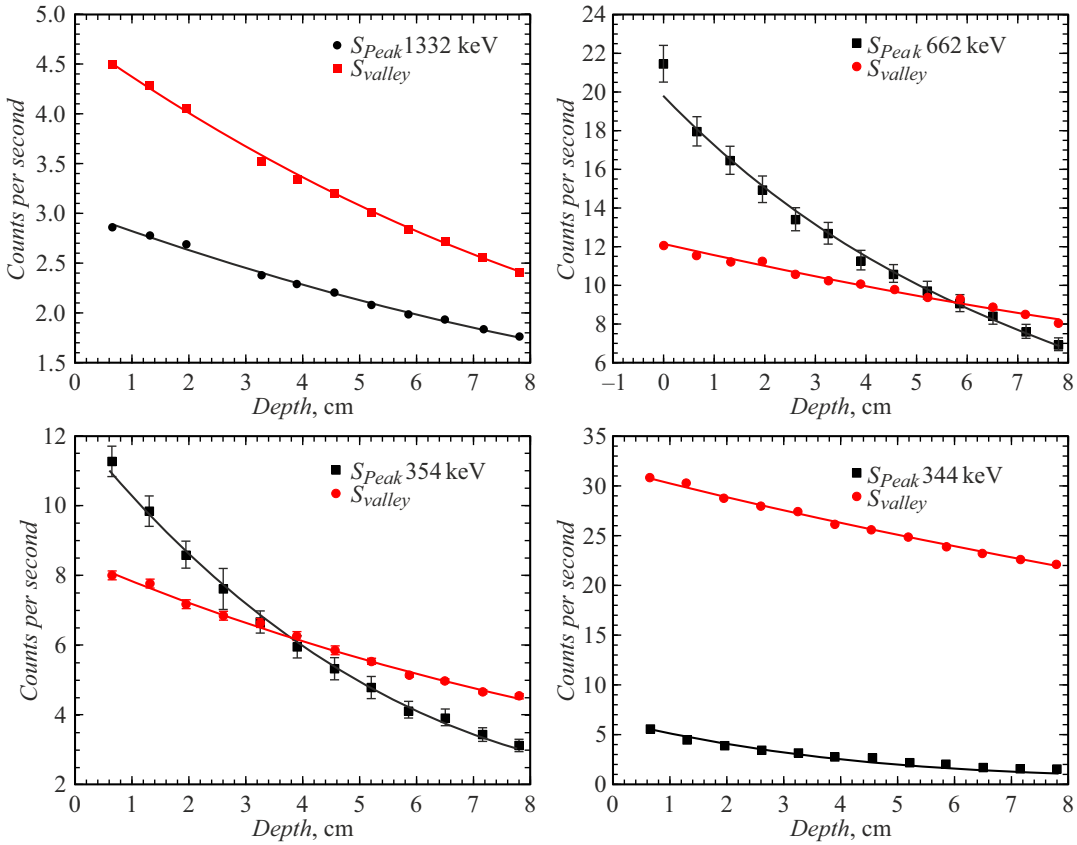

Figure 8. Compton valley areas S_{valley} ^{60}Co, ^{137}Cs, ^{152}Eu, ^{133}Ba and full absorption peak S_{Peak} versus ceramics thickness.

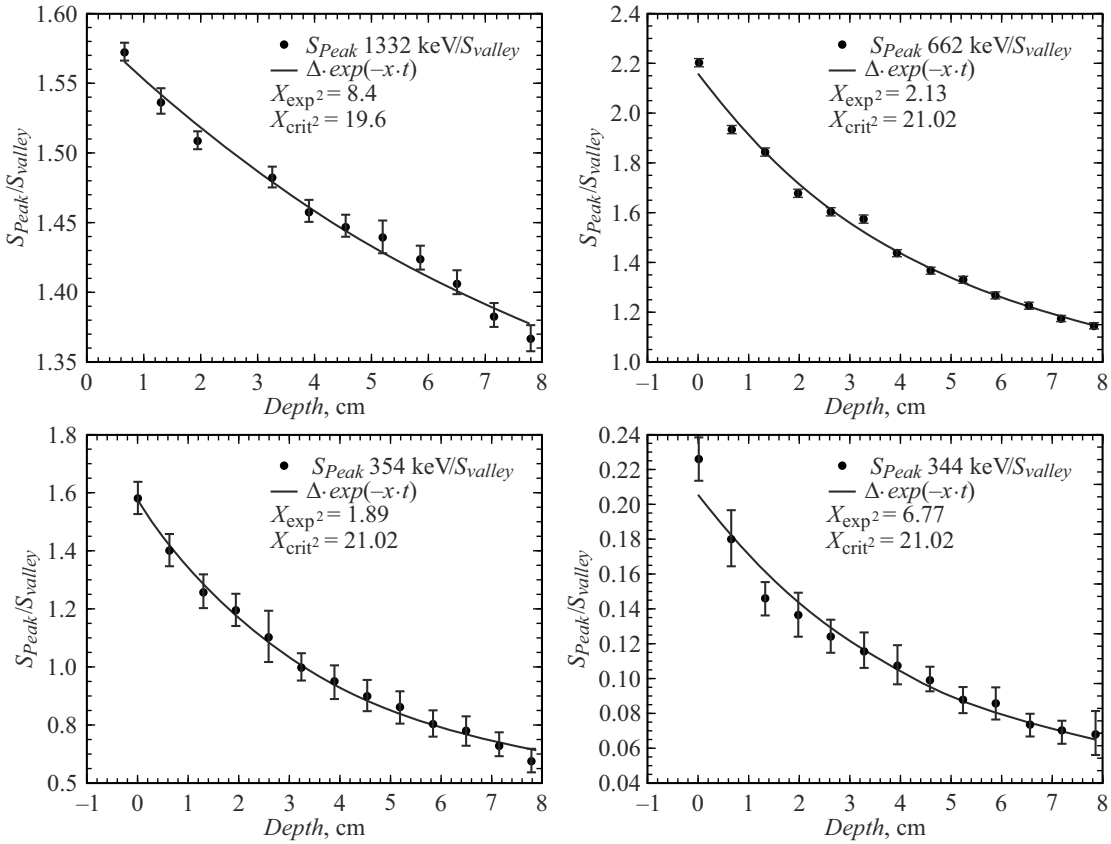

Figure 9. Full absorption peak area and Compton valley S_{Peak}/S_{valley} versus ceramics layer thickness for various sources of gamma-radiation ^{60}Co, ^{137}Cs, ^{133}Ba, ^{152}Eu.

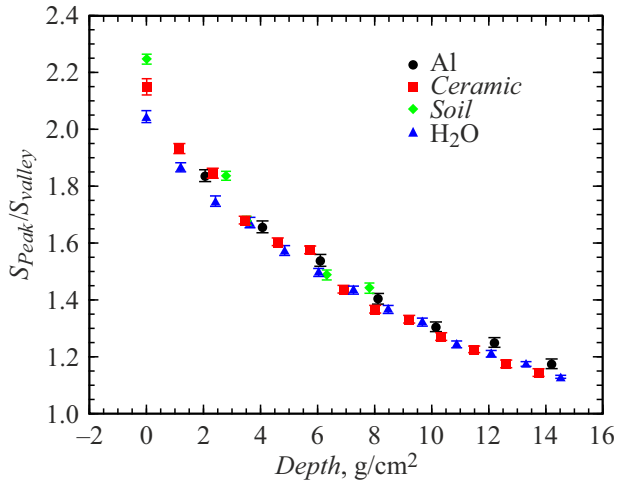

Figure 10. Curves of the ratio of the full absorption peak area counting rate for gamma-ray energy 662 keV to the rate of Compton valley counting rate versus thickness of various absorbers (ceramics, aluminum, soil, water) obtained from experiments.

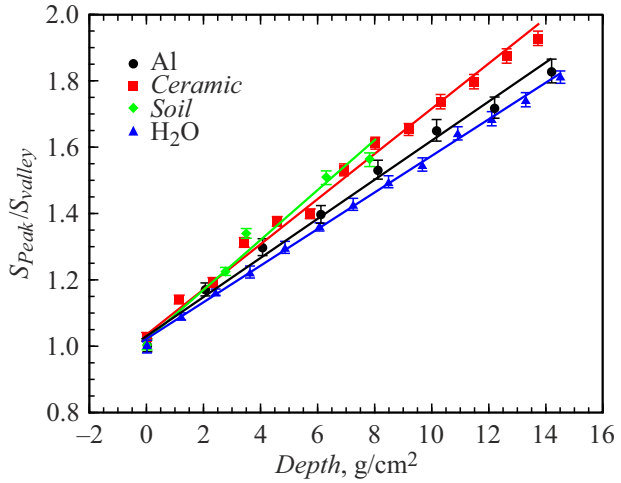

Figure 11. Curves of dependences of inverse normalized ratio of peak–valley for gamma-ray energy 662 keV on the thickness of various absorbers (ceramics, aluminum, soil, water) obtained from experiments.

Table 5. Error of the occurrence depth of ^{137}Cs source in different materials

Material	Depth, cm	Error of depth, cm	Relative error, %
Aluminum (Al)	5.3	0.58	10
Ceramics	7.8	0.32	4.2
Soil	20.0	0.35	1.8
Water (H_2O)	12.0	0.33	2.7

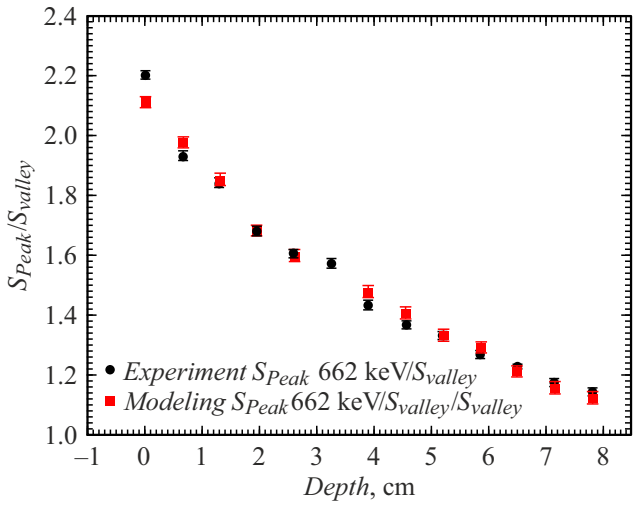

Figure 12. Curves of the ratio of the full absorption peak area counting rate for gamma-ray energy 662 keV to the rate of Compton valley counting rate versus thickness of absorber (ceramics).

cological examination of the environment and assessing the consequences of nuclear man-made disasters.

Funding

This study was performed supported by the strategic academic leadership program „PRIORITY-2030".

Conflict of interest

The authors declare that they have no conflict of interest.

References

[1] M.J. Joyceatal. *Finding the depth of radioactivity in construction materials.* Proceed. Institution of Civil Engineers: Energy, **2** (166), 67 (2018). DOI: 10.1680/ener.12.00003

[2] B. Lee, Y. Kim, W. L'yi, J. Kim, B. Seo, S. Hong. Appl. Radiation and Isotopes, **169** (3), 109558 (2021). DOI: 10.1016/j.apradiso.2020.109558

[3] A.S. Novikov, S.E. Ulin, V.V. Dmitrenko, Z.M. Uteshev, K.F. Vlasik, V.M. Grachev, Y.V. Efremenko, I.V. Chernysheva, A.E. Shustov. Opt. Eng., **53** (2), 021108 (2013). DOI: 10.1117/1.OE.53.2.021108

[4] I.A. Yujakov, A.I. Madzhidov, V.V. Dmitrenko, S.E. Ulin, K.F. Vlasik, V.M. Grachev, R.R. Egorov, K.V. Krivova, Z.M. Uteshev, I.V. Chernysheva, A.E. Shustov. Phys. Part. Nuclei Lett., **21**, 739 (2024). DOI: 10.1134/S154747712470122X

[5] A.I. Madzhidov, V.V. Dmitrenko S.E. Ulin, V.M. Grachev, K.F. Vlasik, R.R. Egorov, M.G. Korotkov, K.V. Krivova, Z.M. Uteshev, I.V. Chernysheva, A.E. Shustov. J. Phys.: Conf. Ser., **2642**, 012011 (2023). DOI: 10.1088/1742-6596/2642/1/012011

[6] I.F. Khimmatov, S.E. Ulin. Phys. Atom. Nuclei, **87**, 620 (2024). DOI: 10.1134/S1063778824700601
[7] A.I. Majidov, V.V. Dmitrienko, S.E. Ulin, V.M. Grachev, D.N. Vlasov, R.R. Egorov, K.V. Krivova, Z.M. Uteshev, A.E. Shustov. Radioaktivniye otkhody, **1** (26), 26 (2024) (in Russian). DOI: 10.25283/258-9707-2024-1-26-34
[8] O. Morris, C. Kanali, Z.C.A. Gariy, E. Ronoh. Intern. J. IT, Engineer. Appl. Sci. Res. (IJIEASR), **7** (7), 1 (2018).
[9] *International Atomic Energy Agency Vienna* (Austria) N.D.S. XMuDat: Photon attenuation data on PC Version 1.0.1 of August 1998 Summary documentation 1998. C. 2.
[10] Vu Ngoc Ba, Truong Thi Hong Loan, Ngo Quang Huy. J. Radioanalytical Nuclear Chem., **317** (3), 1455 (2018). DOI: 317.10.1007/s10967-018-6035-6
[11] GEANT4 TOOLKIT Electronic source: *Articles — substance interaction modelling suite* Available at: http://geant4.cern.ch

Translated by T.Zorina